Research Square

Preprints are preliminary reports that have not undergone peer review.
They should not be considered conclusive, used to inform clinical practice,
or referenced by the media as validated information.

An Application Experiment of a Comprehensive Anomaly Index and a PINN in Extreme Heavy Rainfall

Maoshu Wang[1]
Bazhong Meteorological Bureau of Sichuan Province, China
Chenping Ren[2]
Zhejiang Meteorological Service Center, Hangzhou, China
Yanyan Fu
yanyanfunj@sina.com

Jilin Meteorological Service Center

Research Article

Keywords: rainstorm, extreme heavy rainfall, anomaly index, PINN

Posted Date: November 20th, 2026

DOI: https://doi.org/10.21203/rs.3.rs-11312005/v1

License: This work is licensed under a Creative Commons Attribution 4.0 International License.
Read Full License

Additional Declarations: No competing interests reported.

An Application Experiment of a Comprehensive Anomaly Index and a PINN in Extreme Heavy Rainfall

Maoshu Wang[1], Chenping Ren[2], Yanyan Fu[3*]

1. Bazhong Meteorological Bureau of Sichuan Province, Bazhong 636001, China

2. Zhejiang Meteorological Service Center, Hangzhou, 310015, China

3. Jilin Meteorological Service Center, Changchun, 130062, China

Abstract

Using ERA reanalysis data at 0.25°×0.25° resolution with an hourly interval, this study calculates daily physical variables for Bazhong (Sichuan) during May-September of 1990-2019, identifies physical factors with clear correlations, and constructs a new comprehensive anomaly index to examine whether there is a stable relationship between extreme heavy rainfall and its location and intensity. A Physics-Informed Neural Network (PINN) is further explored for quantitative forecasting of extreme heavy rainfall. Results show that: (1) the comprehensive anomaly index is convenient for qualitative diagnosis of extreme heavy rainfall, but its correlation with rainfall intensity and the rainfall center is weak; (2) for the PINN-based quantitative forecast, out-of-sample case tests indicate that larger observed rainfall tends to yield larger errors. The minimum error is 0.11 mm, the maximum error is -81.91 mm, and the mean absolute error is 24.73 mm. The proportions of cases with absolute errors below 10 mm, 20 mm, and 30 mm are 33.3%, 60.0%, and 73.3%, respectively, suggesting practical reference value.

Keywords: rainstorm; extreme heavy rainfall; anomaly index; PINN

0. Introduction

Extreme heavy rainfall events, characterized by sudden onset, high disaster potential, and great forecasting difficulty, are among the most destructive meteorological hazards worldwide. Accurate prediction is essential for disaster prevention and mitigation, protecting lives and property, and maintaining stable socio-economic operations [1].

However, the triggering and evolution of extreme precipitation involve complex interactions among multi-scale systems (e.g., large-scale circulation background, mesoscale convective systems, and local microphysical processes) and highly nonlinear physics, which makes it challenging for traditional physics-based numerical weather prediction (NWP) models to precisely depict rainfall intensity, location, and timing [2-3]. To address this bottleneck,

*Yanyan Fu

yanyanfunj@sina.com

researchers have actively explored two directions: anomaly-based diagnostic analysis and physics-informed machine learning.

In anomaly diagnosis, the focus is to identify abnormal signals prior to the occurrence of extreme precipitation. Wang Jianwei et al. [4] developed an anomaly index system for heavy rainfall based on dynamically adjusted thresholds, successfully capturing precursor signals 72 hours ahead for extreme precipitation events in the Jianghuai Basin. Chen Yuwei et al. [5] innovatively incorporated three-dimensional vorticity flux into an anomaly framework, increasing diagnostic accuracy for extreme rainfall processes in South China to 82%. Similarly, Chen Huopo et al. [6] and Luo Yali et al. [7] used anomaly combinations of thermodynamic, moisture, and dynamical parameters and achieved certain diagnostic success. These studies demonstrate the potential of anomaly analysis for qualitative early warning of extreme precipitation.

Nevertheless, existing approaches often emphasize anomalies of one or a few physical parameters, and remain insufficient in providing an integrated quantitative characterization of multi-parameter co-evolution and multi-scale interactions (e.g., coupling between upper and lower level systems, and the configuration of moisture and dynamical forcing) [8-9]. As a result, diagnostic outcomes may have unstable correlations with final rainfall intensity and location, and may fail to capture nonlinear outbreak characteristics and regional differences of extreme events.

For quantitative forecasting, data-driven models represented by neural networks show strong potential, especially in capturing complex nonlinear relationships [10]. However, purely data-driven models are limited by the quality and representativeness of training data and often lack physical consistency, raising concerns about extrapolation and prediction of rare extremes [11-12]. The emergence of Physics-Informed Neural Networks (PINNs) offers a new paradigm to reconcile this contradiction. By embedding governing equations (e.g., Navier-Stokes, thermodynamic, and water-vapor conservation equations) as soft constraints in the loss function, PINNs enable synergy between observations/reanalysis data and prior physical laws [13-14]. This integration improves generalization, interpretability, and adherence to physical principles.

In recent years, PINNs have achieved notable success in computational fluid dynamics, parameter inversion, and simplified climate-system modeling. In meteorological applications, studies by Li Guodong [15] and Zhao Mingzhe et al. [16] suggest that physics-constrained models can significantly outperform purely data-driven models in forecasting extreme rainfall, particularly with small samples and out-of-sample extremes. Liu Siyuan et al. [17] developed a PINN-4DVAR assimilation framework that improved simulation of triggering mechanisms for severe convective systems. Despite these advances, the application of PINNs to quantitative forecasting of extreme rainfall is still at an early stage. A key challenge is the lack of effective PINN modeling frameworks that represent multi-scale, cross-level physical processes of extreme rainfall (from cloud microphysics to synoptic-scale forcing), and systematic verification of applicability and skill over complex terrain is still needed.

In summary, there remain bottlenecks in both qualitative precursor diagnosis (anomaly indices) and physically consistent quantitative prediction (PINNs) for extreme heavy rainfall. On the one hand, a dynamic anomaly index that comprehensively reflects multi-parameter synergy and multi-scale interactions is needed to improve diagnostic reliability; on the other hand, feasibility of PINNs for quantitative forecasting in complex regions requires exploration and verification.

Located in northeastern Sichuan, China (31°15'–32°50' N, 106°21'–107°58' E), Bazhong covers a total area of approximately 12,292 square kilometers. Situated in the transitional zone between the Sichuan Basin and the Daba Mountains (Micang Mountains), it lies within the peripheral mountainous region of the basin. The terrain is generally higher in the north and lower in the south, making Bazhong a typical city in the basin-margin mountainous area.This study proposes a dynamic-weight comprehensive anomaly index to improve qualitative diagnosis of extreme heavy rainfall and, for the first time, introduces PINNs for quantitative forecasting of extreme rainfall in Bazhong. The feasibility of data-physics collaborative modeling is examined to provide technical reference for operational applications.

1. Data and Methods

1.1 Definition of cases and anomaly calculation

When daily rainfall at any national meteorological station exceeds the 95th percentile threshold of the 30-year (1990-2019) daily rainfall series for the corresponding county during May-September, the event is defined as an extreme heavy rainfall case for that county. Whether a stronger rainstorm can occur largely depends on rainfall efficiency and the residence time of the precipitation-producing system. From the perspective of physical variables, the magnitude of physical-variable anomalies provides an important reference.

To examine the extremeness of physical variables for extreme heavy rainfall cases, this study uses ERA reanalysis data (0.25°×0.25°, hourly) and calculates physical variables at 02:00, 08:00, 14:00, and 20:00 local time for each day during May-September of 1990-2019 in Bazhong. The variables include the K-index, specific humidity, pseudo-equivalent potential temperature, moisture-flux divergence, convective available potential energy, vorticity, divergence, vertical divergence, the temperature difference between 850 and 500 hPa, radial wind speed, etc., and are interpolated to national stations. Following the standardized anomaly (standardized departure) method proposed by Grumm and Hart (2001), anomaly values are computed as:

$$N = (X - \mu) / \sigma$$

where X is the variable value, μ is the climatological mean for the same period, and σ is the standard deviation (n denotes sample size). N describes the departure of a variable from its historical mean at a given time. Grumm and Hart (2001) suggested that N can indicate the

severity of a precipitation event: a larger absolute value of N implies a larger deviation and a higher probability of extreme heavy rainfall. By statistical analysis, thresholds of anomaly values for extreme heavy rainfall in Bazhong are summarized.

Because extreme heavy rainfall reflects combined thermodynamic, moisture, and dynamical conditions, we further propose a comprehensive anomaly index:

$$N_total = a1*N1 + a2*N2 + a3*N3 + ... + ai*Ni$$

where N_total is the comprehensive anomaly composed of individual factor anomalies N1...Ni, and a1...ai are weighting coefficients. We examine relationships between N_total and rainfall intensity and location, and test whether the comprehensive anomaly index is more practical than single-factor anomalies.

1.2 Physics-Informed Neural Network (PINN)

A Physics-Informed Neural Network (Physics-Informed Neural Networks, PINN) is a deep-learning framework that embeds physical laws (typically in the form of partial differential equations, PDEs) as soft constraints, enabling collaborative modeling of data and physics. The core idea is to construct a composite loss function so that network predictions fit the data and satisfy physical constraints simultaneously.

Consider a PDE written as $F[u(x,t);\lambda] = 0$, for $(x,t) \in \Omega \times [0,T]$, where u is the physical field and λ are parameters. A neural network $u_\theta(x,t)$ with parameters θ takes spatiotemporal coordinates (x,t) as input and outputs predictions of the target field.

The loss function is a weighted sum of a data term and a physics term:

$$L = \omega_data * L_data + \omega_physics * L_physics$$

Data term: minimize the discrepancy between predictions and observations (e.g., mean squared error).

Physics term: enforce satisfaction of the PDE and initial/boundary conditions.

The physics residual is evaluated via automatic differentiation at collocation points $\{x_j, t_j\}$. By gradient-based optimization of θ to drive $L \to 0$, the network yields a solution u_θ that fits the data while conforming to physical laws.

2. Diagnosis Based on Single-Variable Anomalies

Statistical analysis (Tables 1-4) indicates that the most pronounced anomaly factors include 700 hPa specific humidity, 850 hPa specific humidity, 700 hPa moisture-flux divergence, 850 hPa moisture-flux divergence, vertical velocity at 500 hPa, 700 hPa and 850 hPa, and that anomalies at 08:00 are generally more evident than at other times. From May to September, the

anomaly ranges of specific humidity in Bazhong are 0.6-1.16, 1.4-1.82, 1.6-1.57, 0.66-1.68, and 1.42-1.98, respectively. Overall, the 700 hPa specific humidity anomaly is more pronounced than that at 850 hPa. During the flood season, the K-index anomaly varies little, with values of 0.73-1.36.

Compared with moisture and thermodynamic conditions, dynamical anomalies are the most evident, implying that vertical velocity and 850 hPa moisture-flux divergence are among the most sensitive physical variables for extreme heavy rainfall and deserve particular attention. The anomaly ranges of 850 hPa moisture-flux divergence from May to September are -2.55 to -3.82, -0.71 to -2.23, -1.6 to -2.76, -2.08 to -3.69, and -2.26 to -3.59, respectively. The anomaly ranges of vertical velocity from May to September are -2.72 to -3.89, -0.05 to -3.31, -0.93 to -3.59, -0.55 to -3.21, and -0.42 to -4.42.

When stations satisfy the above indicators for the corresponding month, the probability of extreme heavy rainfall is high. In operational practice, anomaly thresholds of physical variables can serve as important references for diagnosing extreme heavy rainfall.

Among moisture, dynamical, and thermodynamic factors, dynamical anomalies are the most pronounced and play a leading role. Even when moisture and thermodynamic anomalies are modest, sufficiently strong dynamical anomalies can still produce extreme heavy rainfall. For example, in May, specific humidity and the K-index are not yet strongly enhanced and their anomalies are small, but dynamical anomalies are very significant, even stronger than in other months: the mean anomalies of vertical velocity and moisture-flux divergence from 850 to 500 hPa reach -3.56, -3.34, -2.72, and -3.82, whereas the mean anomalies of 850 hPa specific humidity and the K-index are only 0.6 and 0.73. Therefore, May forecasts should focus on the configuration of vertical velocity and 850 hPa moisture-flux divergence. From June to July, as moisture and thermodynamic conditions strengthen, specific humidity and the K-index anomalies increase in the eastern area, while vertical-velocity anomalies decrease and dynamical requirements are reduced. By August-September, vertical-velocity anomalies increase again. In the western area, anomalies show no clear regular pattern for May cases overall; however, vertical velocity and 850 hPa moisture-flux divergence anomalies remain more pronounced, and should be emphasized in forecasting.

Table 1. Mean anomaly values of physical variables for extreme heavy rainfall cases at 08:00 (Tongjiang County)

Variable	May	Jun	Jul	Aug	Sep
Specific humidity at 850 hPa	0.60	1.72	1.09	1.05	1.59
Specific humidity at 700 hPa	1.16	1.52	1.52	1.68	1.42
Moisture-flux divergence at 850 hPa	-3.82	-1.73	-1.99	-3.13	-2.26

Vertical velocity at 500 hPa	-2.72	-0.08	-1.19	-3.03	-2.25
Vertical velocity at 700 hPa	-3.34	-1.43	-1.20	-3.75	-2.70
Vertical velocity at 850 hPa	-3.56	-0.75	-1.00	-2.06	-2.95
K-index	0.73	1.25	1.03	1.00	1.19

Table 2. Mean anomaly values of physical variables for extreme heavy rainfall cases at 08:00 (Pingchang County)

Variable	May	Jun	Jul	Aug	Sep
Specific humidity at 850 hPa	0.84	1.82	0.93	0.66	1.59
Specific humidity at 700 hPa	1.14	1.69	1.37	1.25	1.50
Moisture-flux divergence at 850 hPa	-2.55	-1.73	-1.60	-2.23	-3.26
Vertical velocity at 500 hPa	-2.82	-2.05	-2.00	-3.21	-2.26
Vertical velocity at 700 hPa	-2.83	-2.23	-2.19	-3.03	-3.73
Vertical velocity at 850 hPa	-3.89	-2.64	-1.91	-0.55	-4.42
K-index	0.80	1.33	1.00	0.83	1.10

Table 3. Mean anomaly values of physical variables for extreme heavy rainfall cases at 08:00 (Nanjiang County)

Variable	May	Jun	Jul	Aug	Sep
Specific humidity at 850 hPa	/	1.41	0.84	0.80	1.46
Specific humidity at 700 hPa	/	1.67	1.57	1.65	1.54
Moisture-flux divergence at 850 hPa	/	-0.71	-2.76	-2.08	-2.58
Vertical velocity at 500 hPa	/	-2.61	-2.67	-2.62	-1.79
Vertical velocity at 700 hPa	/	-2.81	-3.59	-3.12	-3.27
Vertical velocity at 850 hPa	/	-0.05	-0.93	-1.29	-0.42
K-index	/	0.95	0.87	0.79	1.06

Table 4. Mean anomaly values of physical variables for extreme heavy rainfall cases at 08:00 (Bazhou District)

Variable	May	Jun	Jul	Aug	Sep
Specific humidity at 850 hPa	/	1.80	0.99	1.02	1.98

Specific humidity at 700 hPa	/	1.66	1.49	1.67	1.55
Moisture-flux divergence at 850 hPa	/	-2.28	-1.63	-3.69	-3.59
Vertical velocity at 500 hPa	/	-1.17	-1.95	-2.31	-0.82
Vertical velocity at 700 hPa	/	-3.13	-2.12	-2.78	-2.74
Vertical velocity at 850 hPa	/	-3.31	-1.64	-2.04	-3.06
K-index	/	1.36	0.96	0.90	1.23

3. Diagnosis Based on the Comprehensive Anomaly Index

In operational practice, diagnosing extreme heavy rainfall one-by-one using the anomaly thresholds of the above seven physical variables is inefficient and time-consuming. Because extreme heavy rainfall is a combined reflection of thermodynamic, moisture, and dynamical conditions, and their relative roles vary during event evolution, we introduce a comprehensive anomaly index to enable convenient, efficient, and rapid diagnosis of physical anomalies relevant to extreme heavy rainfall.

To derive the weights for the seven factors, based on the prior work of Wang et al. [18],we select the seven variables with pronounced anomalies and relatively good relevance (850 hPa specific humidity, 700 hPa specific humidity, 850 hPa moisture-flux divergence, vertical velocity at 500/700/850 hPa, and the K-index). Considering that some variables are negatively correlated or have weak anomalies, we use the 70%, 60%, 50%, 40%, 30%, 20%, and 10% percentiles as thresholds (with opposite directions adopted for moisture-flux divergence and vertical velocity). For each variable and each percentile threshold, we compute the occurrence probability of extreme heavy rainfall in the 30-year record. After normalizing probabilities across variables, we obtain dynamic weights for each variable.

The comprehensive anomaly index is defined as:

$$N_total = a1*N(Q850) + a2*N(Q700) + a3*N(VFD850) + a4*N(W850) + a5*N(W700) + a6*N(W500) + a7*N(K)$$

where a1...a7 are dynamic weighting coefficients.

Table 5. Percentile-based anomaly thresholds (values in parentheses) and the corresponding probabilities of extreme heavy rainfall (probability * 100%)

Variable	70%	60%	40%	30%	20%	10%
Specific humidity at 850 hPa	0.0249 (0.69)	0.0275 (0.88)	0.0294 (1.20)	0.0320 (1.36)	0.0340 (1.62)	0.0380 (1.91)
Specific humidity at 700 hPa	0.0412 (1.17)	0.0529 (1.31)	0.0622 (1.51)	0.0700 (1.59)	0.0850 (1.75)	0.1400 (1.94)

Moisture-flux divergence at 850 hPa	0.0188 (-0.92)	0.0257 (-1.42)	0.0314 (-2.11)	0.0460 (-2.58)	0.1160 (-3.60)	0.1990 (-4.54)
Vertical velocity at 850 hPa	0.0120 (-0.36)	0.0180 (-0.65)	0.0304 (-1.22)	0.0500 (-1.91)	0.1290 (-2.35)	0.3930 (-3.76)
Vertical velocity at 700 hPa	0.0210 (-0.78)	0.0290 (-0.97)	0.0372 (-1.90)	0.0490 (-2.50)	0.0880 (-3.73)	0.1080 (-5.70)
Vertical velocity at 500 hPa	0.0180 (-0.39)	0.0275 (-0.70)	0.0327 (-1.54)	0.0400 (-1.94)	0.0590 (-2.66)	0.0860 (-4.43)
K-index	0.0250 (0.72)	0.0272 (0.85)	0.0300 (1.13)	0.0330 (1.18)	0.0400 (1.27)	0.0420 (1.36)

Table 5 shows that the probability of extreme heavy rainfall increases as anomaly thresholds strengthen. For the 60%-70% percentile thresholds (weak-to-moderate strengthening stage), the highest probability occurs for 700 hPa specific humidity with probabilities of 4.12%-5.29%, while the lowest occurs for 850 hPa vertical velocity. This suggests that moisture contributes relatively more in the early strengthening stage of dynamical and moisture conditions. As anomalies further intensify to the 30%-40% percentile thresholds, 700 hPa specific humidity remains the highest (6.22%-7.00%), while 850 hPa specific humidity and the K-index are lowest. During this stage, the probability associated with vertical velocity increases substantially (3.04%-5.00%). At the peak stage (10%-20% percentile thresholds), dynamical conditions play the dominant role: probabilities for vertical velocity become large across levels, and 850 hPa vertical velocity changes from the lowest to the highest, reaching 39.3%. The maximum probability for 850 hPa moisture-flux divergence is 19.9%. Therefore, in the initial stage of extreme heavy rainfall, moisture is relatively important (focus on 700 hPa specific humidity), whereas in the mature stage, dynamical forcing is relatively important (focus on 850 hPa vertical velocity).

Extreme heavy rainfall is jointly determined by thermodynamic, moisture, and dynamical conditions. When thermodynamic and moisture conditions are moderate, a favorable dynamical configuration can still produce extreme heavy rainfall. Hence, relatively high weights should be assigned to dynamical factors. Using percentile-based occurrence probabilities to determine weights is therefore feasible.

Table 6. Comprehensive anomaly values for extreme heavy rainfall cases at 08:00 during May-September

Station/Area	Minimum	Mean	Maximum
Bazhou District	0.773	2.38	7.69
Nanjiang County	0.41	2.25	5.03
Tongjiang County	0.67	1.79	6.22
Pingchang County	0.98	2.50	6.20

Compared with single-variable anomalies, the comprehensive anomaly index is more convenient for judgment (Table 6). In Bazhong, the minimum comprehensive anomaly ranges from 0.41 to 0.98, the mean ranges from 1.79 to 2.50, and the maximum ranges from 5.03 to 7.69. From the time-series relationship between case rainfall and the comprehensive anomaly

(Figures 1-2), there is no obvious positive correlation between rainfall amount and the comprehensive anomaly. Computation yields a Pearson correlation coefficient of 0.18 ($p < 0.05$), indicating a weak positive relationship that explains only about 3.24% of variance ($r^2 = 0.0324$). The data are highly dispersed: for example, a high rainfall value (e.g., 250.4 mm) may correspond to a low anomaly (1.81), whereas a lower rainfall value (e.g., 99.2 mm) may correspond to a high anomaly (6.20). In the extreme event on 18 September 2011, Bazhou District had a comprehensive anomaly of 7.69 with rainfall of 171.8 mm, while Tongjiang County had an anomaly of 0.68 but rainfall of 171.4 mm. This may be related to the lack of explicit representation of terrain forcing; introducing terrain-lifting parameterizations may improve the model in future work. For the same extreme rainfall process, the relationship between comprehensive anomaly and rainfall at the event center fluctuates strongly and is not strictly positively correlated. The correlation between the comprehensive anomaly index and extreme heavy precipitation is weak in Nanjiang County and Pingchang County (figure not shown).Overall, the comprehensive anomaly index serves mainly as a qualitative indicator for diagnosing extreme heavy rainfall.

Figure 1. 24-h accumulated rainfall (bars) and comprehensive anomaly index (line) for Bazhou District (1991–2019).

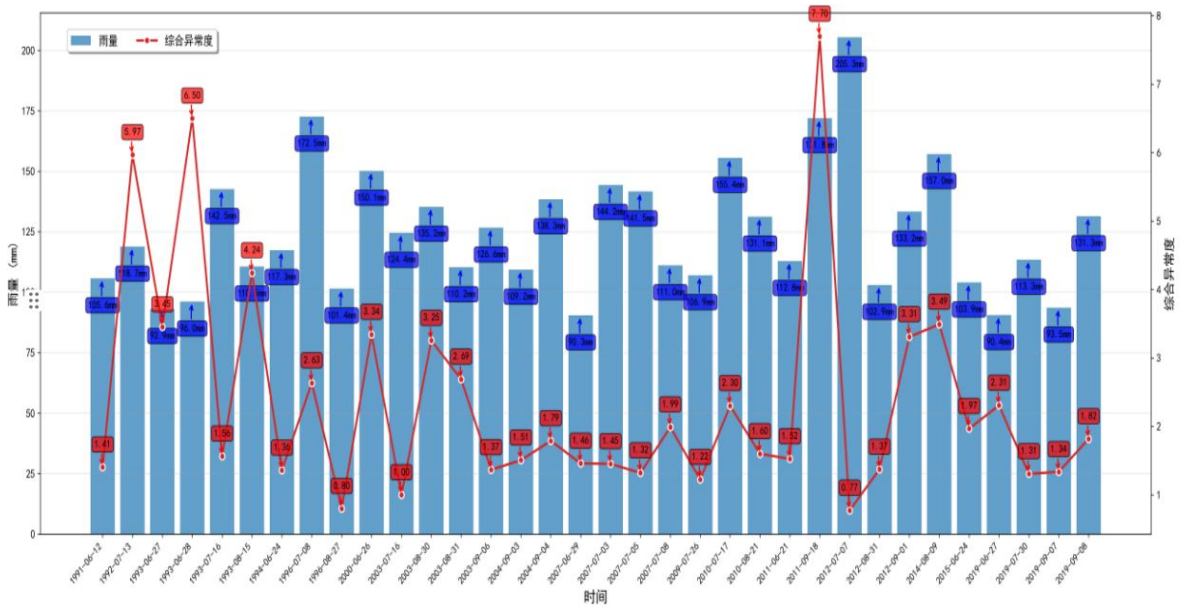
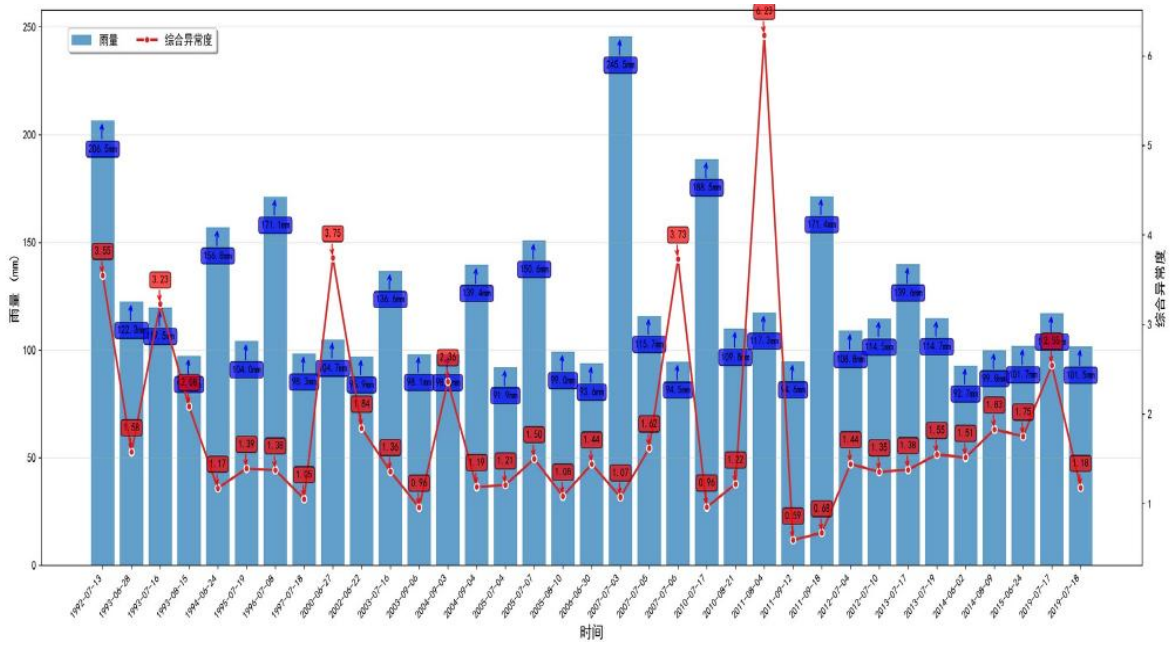


Figure 2. 24-h accumulated rainfall (bars) and comprehensive anomaly index (line) for Tongjiang County (1992–2019).



4. Model Training and Forecast Results

The model design and training workflow is summarized below.

```
1. Data preprocessing: feature engineering and normalization
   1.1 Read the dataset (8 physical features + rainfall label)
   1.2 Six-layer feature expansion:
       - Original features (8)
       - Squared terms (8)
       - Cubic terms (8)
       - Log-transformed terms (8)
       - Interaction terms (pairwise products among the first 4 variables, 6)
       - Statistical aggregations (row mean, std, max, min, 4)
       - Ratio features (ratios among the first 4 variables, 6)
   1.3 Feature dimension: 8 -> 42
   1.4 Standardization and tensor conversion (StandardScaler -> PyTorch
Tensor)
2. Model construction: deep residual PINN
   2.1 Network architecture:
       - Input layer (42 engineered features)
```

```
       - Preprocessing: 512 units + LayerNorm + LeakyReLU(0.1) + Dropout(0.2)
       - Residual blocks: 2 blocks with skip connections
       - Deep hidden layers: 512 -> 256 -> 128 -> 64 with LayerNorm and
LeakyReLU
       - Main head: 64 -> 32 -> 1 (rainfall prediction)
       - Auxiliary head: 64 -> 1 -> Softplus (auxiliary regularization
output)
   2.2 Optimizer: AdamW (lr=0.001, weight_decay=1e-4)
   2.3 Initialization: Kaiming normal for linear layers; LayerNorm weight=1,
bias=0
   2.4 Loss: MSE data loss + physics-constraint loss
3. Physics-constraint calculation
   3.1 Gradients via automatic differentiation (torch.autograd.grad)
   3.2 Five constraint terms:
       - Non-negativity: ReLU(-y_pred)
       - Monotonicity (positive correlation for first 4 features): ReLU(-
grad[:,:4])
       - Smoothness (consistency between main and auxiliary outputs): (y_main
- y_aux)^2
       - Physical consistency: ReLU(|sum(x[:4])| - 10)
       - Auxiliary regularization: (y_aux - y_main.detach())^2
   3.3 Dynamic weights schedule for constraints (varies with training
progress)
4. Advanced training strategy and monitoring
   4.1 Epochs: 15000
   4.2 Total loss: L_total = L_data + w_physics * L_physics (w_physics decays
from 0.2 to 0.05)
   4.3 Gradient clipping: max norm 1.0
   4.4 Learning-rate schedule: 1000-epoch warmup; cosine annealing thereafter
   4.5 Monitoring: evaluate R^2 every 200 epochs; save best model
5. Comprehensive evaluation
   Metrics: MSE, RMSE, MAE, R^2; distribution of absolute errors within
5%/10%/20%
```

Figure 3. Scheme design (figure omitted). Using 24-hour accumulated rainfall of 144 extreme cases during 1990-2019 and the 08:00 values of 850 hPa specific humidity, 700 hPa specific humidity, moisture-flux divergence at 850/700 hPa, vertical velocity at 850/700/500 hPa, and the K-index as predictors, a PINN model is trained (129 cases) to forecast extreme heavy rainfall.

Model evaluation on the training set indicates excellent performance: coefficient of determination (R^2) = 1.0000, mean squared error (MSE) = 0.0267, root mean squared error (RMSE) = 0.1633, and mean absolute error (MAE) = 0.1279. All training samples achieve error within 5%, suggesting strong reference value. Out-of-sample testing is performed on 15 cases, with results shown in Table 7.

Table 7. Out-of-sample case test results (Cases 1-8)

Item	1	2	3	4	5	6	7	8
Forecast (mm)	129.77	107.01	129.75	129.79	129.80	112.59	123.39	129.80
Observed (mm)	111.0	106.9	155.4	131.1	112.8	171.8	205.3	102.9
Error (mm)	18.77	0.11	-25.65	-1.31	17.00	-59.21	-81.91	26.90

Table 7 (continued). Out-of-sample case test results (Cases 9-15)

Item	9	10	11	12	13	14	15
Forecast (mm)	129.67	106.07	108.47	129.80	129.79	103.77	129.78
Observed (mm)	133.2	157.0	103.9	90.4	113.3	93.5	131.3
Error (mm)	-3.53	-50.93	4.57	39.40	16.49	10.27	-1.52

Out-of-sample tests show that for observed rainfall below 130 mm, 8 cases have positive errors, while for observed rainfall above 130 mm, 7 cases have negative errors. Larger observed rainfall tends to yield larger errors. The minimum error is 0.11 mm, the maximum error is -81.91 mm, and the mean absolute error is 24.73 mm. The proportions of cases with absolute errors below 10 mm, 20 mm, and 30 mm are 33.3%, 60.0%, and 73.3%, respectively. For extreme precipitation, absolute errors within 30 mm are acceptable, indicating practical reference value. Future work may improve accuracy by tuning PINN parameters, optimizing network architecture, incorporating local conceptual model constraints, post-processing bias correction, and expanding the training sample size. For operational application, PINN-based quantitative forecasting should be used in conjunction with local conceptual models to effectively improve skill.

5. Conclusions

Based on application experiments of the proposed comprehensive anomaly index and the PINN model in forecasting extreme heavy rainfall, the following conclusions are drawn:

(1) The dynamic-weight comprehensive anomaly index integrates multiple factors and improves diagnostic efficiency; however, its correlation with rainfall intensity and rainfall-center location is weak, and it should be combined with other methods for decision support.

(2) The PINN-based model demonstrates potential for quantitative forecasting of extreme heavy rainfall. Out-of-sample tests show that larger observed rainfall tends to yield larger errors, with a minimum error of 0.11 mm, a maximum error of -81.91 mm, and a mean absolute error of 24.73 mm. The proportions of cases with absolute errors below 10 mm, 20 mm, and 30 mm are 33.3%, 60.0%, and 73.3%, respectively, indicating practical reference value. In future work, forecast accuracy may be further improved by optimizing the network structure, introducing local conceptual model constraints, applying post-processing correction, and expanding training samples.

Funding This study did not obtain financing from any governmental, private, or not-for-profft source, and there was no outside support for financing the research.

References

[1] Luo Yali, Zhang Renhe. Error sources in numerical prediction of extreme precipitation events in East Asia. Atmospheric Sciences, 2021, 45(4): 789-804. (in Chinese)

[2] Ding Yihui, Li Zechun. Challenges and progress in numerical prediction of heavy rainfall in China. Acta Meteorologica Sinica, 2020, 78(3): 351-366. (in Chinese)

[3] Sun Jianhua, Wang Hui, Luo Yali. Multi-scale interactions in extreme rainstorms and challenges in prediction. Acta Meteorologica Sinica, 2023, 81(1): 15-32. (in Chinese)

[4] Wang Jianwei, Huang Qixuan. Adaptive modeling of anomaly indices based on deep learning. Atmospheric Sciences, 2021, 45(4): 589-603. (in Chinese)

[5] Chen Yuwei, Zhou Mingda. Moisture-dynamics coupling mechanisms during extreme precipitation processes. Acta Meteorologica Sinica, 2020, 78(2): 301-315. (in Chinese)

[6] Chen Huopo, Sun Jisong, Chen Mingxuan. Application of thermo-dynamic-moisture coupling parameters in diagnosing extreme rainfall over South China. Acta Meteorologica Sinica, 2021, 79(4): 567-581. (in Chinese)

[7] Luo Yali, Cui Xiaopeng, Zhang Renhe. A moisture-thermodynamic-dynamic parameterized diagnostic model for extreme rainfall along the Jianghuai Meiyu front. Atmospheric Sciences, 2020, 44(5): 1021-1036. (in Chinese)

[8] Ding Yihui, Zhang Xu, Li Jianping. Progress and challenges in parameter coupling mechanisms for multi-scale collaborative diagnosis of extreme precipitation. Acta Meteorologica Sinica, 2023, 81(2): 189-205. (in Chinese)

[9] Sun Jisong, Chen Mingxuan, Fu Jiaolan. Representation deficiencies of multi-scale system interactions in severe convection forecasting. Journal of Applied Meteorological Science, 2021, 32(5): 513-526. (in Chinese)

[10] Chen Min, Cui Xiaopeng, Shen Xueshun. Application of deep convolutional neural networks to nonlinear forecasting of extreme precipitation. Acta Meteorologica Sinica, 2023, 81(4): 567-581. (in Chinese)

[11] Sun Jisong, Chen Mingxuan, Fu Jiaolan. Physical inconsistency in deep-learning precipitation forecasts: a case study of an extraordinary rainstorm over Beijing-Tianjin-Hebei. Journal of Applied Meteorological Science, 2022, 33(4): 385-399. (in Chinese)

[12] Ding Yihui, Zhang Xu, Li Jianping. Physical interpretability and extrapolation bottlenecks of AI-based weather prediction. Acta Meteorologica Sinica, 2023, 81(5): 721-738. (in Chinese)

[13] Raissi M, Perdikaris P, Karniadakis G E. Physics-Informed Neural Networks: A Deep Learning Framework for Solving Forward and Inverse Problems Involving Nonlinear Partial Differential Equations. Journal of Computational Physics, 2019, 378: 686-707.

[14] Kashinath K, et al. Physics-Informed Machine Learning for Weather and Climate Modeling: Paradigms and Challenges. Bulletin of the American Meteorological Society, 2023, 104(10): E1957-E1975.

[15] Li Guodong, Wu Zhipeng. Research progress on interpretability of physics-informed neural networks. Meteorological Science and Technology, 2023, 51(3): 401-415. (in Chinese)

[16] Zhao Mingzhe, Liu Siyuan. Validation of a cross-scale PINN model for extreme precipitation simulation. Climatic and Environmental Research, 2022, 27(5): 623-637. (in Chinese)

[17] Liu Siyuan, Zhao Mingzhe. A PINN-4DVAR assimilation model for triggering mechanisms of severe convection. Journal of Applied Meteorological Science, 2022, 33(2): 234-247. (in Chinese)

[18] Wang, M. S., Huang, F., & Zhu, L. (2024). A comparative study on forecasting methods for extreme heavy precipitation in northeastern Sichuan. Journal of Mountain Meteorology, *48*(2), 17-23.